CHEMISTRY
A European Journal

Supporting Information

Magnetization Blocking in $Fe_2^{III}Dy_2^{III}$ Molecular Magnets: Ab Initio Calculations and EPR Spectroscopy

Veacheslav Vieru,[a] Liviu Ungur,[a, e] Valeriu Cemortan,[a] Andrey Sukhanov,[b] Amer Baniodeh,[c] Christopher E. Anson,[c] Annie K. Powell,*[c, d] Violeta Voronkova,*[b] and Liviu F. Chibotaru*[a]

chem_201803821_sm_miscellaneous_information.pdf

Supporting Information

Ab initio calculations

Table S1. Contractions of the employed basis sets.

Basis 1	Basis 2
Dy.ANO-RCC...7s6p4d3f1g	Dy.ANO-RCC...8s7p5d4f2g1h
Lu.ANO-DK3.Tsuchiya.27s23p15d10f.6s4p3d1f	Lu.ANO-RCC...7s6p4d3f1g
Zn.ANO-RCC...5s4p2d1f	Zn.ANO-RCC...5s4p2d1f
O.ANO-RCC...3s2p1d (close)	O.ANO-RCC...4s3p2d (close)
O.ANO-DK3.Tsuchiya.12s8p.2s1p (distanced)	O.ANO-DK3.Tsuchiya.12s8p.2s1p (distanced)
N.ANO-RCC...3s2p1d (close)	N.ANO-RCC...4s3p2d (close)
N.ANO-DK3.Tsuchiya.12s8p.2s1p (distanced)	N.ANO-DK3.Tsuchiya.12s8p.2s1p (distanced)
C.ANO-RCC...3s2p1d (close)	C.ANO-RCC...4s3p1d (close)
C.ANO-DK3.Tsuchiya.12s8p.2s1p (distanced)	C.ANO-DK3.Tsuchiya.12s8p.2s1p (distanced)
H.ANO-RCC...2s1p (close)	H.ANO-RCC...3s2p (close)
H.ANO-DK3.Tsuchiya.6s.1s (distanced)	H.ANO-DK3.Tsuchiya.6s.1s (distanced)

Table S2. Energies of the lowest Kramers doublets (cm^{-1}) of Dy ions in compound **1**.

Basis 1	Basis 2
0	0
77.202	86.277
114.506	121.877
144.785	149.930
158.113	170.035
209.556	210.450
299.888	295.383
376.622	385.706

Table S3. *g* tensors of the low-lying Kramers doublets (KD) of Dy ions in compound **1**.

KD		Basis 1 *g*	Basis 2 *g*
1	g_X	0.1791	0.1299
	g_Y	0.3015	0.2151
	g_Z	19.1003	19.2019
2	g_X	2.2682	2.0988
	g_Y	6.2593	5.7294
	g_Z	11.2736	11.7101
3	g_X	2.4613	1.7505
	g_Y	2.8489	2.4664
	g_Z	9.6287	11.6118
4	g_X	2.1362	3.5369
	g_Y	3.5597	4.5858
	g_Z	11.6522	11.3039
5	g_X	3.4533	2.5859
	g_Y	3.5453	3.5144
	g_Z	13.8183	15.3944
6	g_X	0.5866	0.6390
	g_Y	0.7516	1.0840
	g_Z	15.5096	15.2445
7	g_X	0.0700	0.0872
	g_Y	0.1799	0.2107
	g_Z	19.1603	19.1196
8	g_X	0.0111	0.0157
	g_Y	0.0490	0.0496

	g_Z	19.6637	19.6577

Table S4. Energies of the lowest Kramers doublets (cm^{-1}) of Dy ions in compound **2**.

Basis 1	Basis 2
0	0
110.817	114.903
169.535	179.913
183.296	188.773
230.295	240.576
264.559	265.791
338.725	332.064
473.688	478.536

Table S5. *g* tensors of the low-lying Kramers doublets (KD) of Dy ions in compound **2**.

KD		Basis 1 *g*	Basis 2 *g*
1	g_X	0.0605	0.0521
	g_Y	0.1018	0.0877
	g_Z	19.4823	19.4985
2	g_X	1.0738	0.9384
	g_Y	1.9183	1.5644
	g_Z	14.8567	15.2696
3	g_X	1.6387	0.5488
	g_Y	2.1077	1.6032
	g_Z	13.7491	14.0648
4	g_X	2.0720	3.2863
	g_Y	3.2205	4.8191
	g_Z	11.9341	9.3819
5	g_X	1.7997	1.2297
	g_Y	3.1995	4.1338
	g_Z	11.8164	10.5140
6	g_X	0.7170	1.2728
	g_Y	1.3966	2.6261
	g_Z	16.0165	15.9853
7	g_X	0.0610	0.1056
	g_Y	0.1012	0.1880
	g_Z	19.2474	19.1933
8	g_X	0.0052	0.0063
	g_Y	0.0104	0.0122
	g_Z	19.7952	19.7867

Table S6. Energies of the lowest Kramers doublets (cm^{-1}) of Dy ions in compound **4**.

Spin-orbit energies, cm^{-1}	
Basis 1	**Basis 2**
0	0
99.537	105.709
139.704	147.762
171.265	176.726
204.796	214.938
256.635	253.712
340.838	332.364
441.536	446.145

Table S7. The *g* tensors of the lowest Kramers doublets (KD) of Dy ions in compound **4**.

KD		Basis 1 *g*	Basis 2 *g*
1	g_X	0.080599	0.061733
	g_Y	0.107794	0.086288
	g_Z	19.401383	19.434836
2	g_X	1.236348	1.110025
	g_Y	3.184877	2.534804
	g_Z	13.950387	14.626564
3	g_X	0.043138	0.697118
	g_Y	1.501803	1.414535
	g_Z	14.627774	16.293962
4	g_X	2.418493	2.633004
	g_Y	3.225411	3.776514
	g_Z	10.481811	10.123479
5	g_X	2.966740	3.107733
	g_Y	3.596238	3.400956
	g_Z	12.842904	13.661295
6	g_X	0.129625	0.176784
	g_Y	0.284032	0.377744
	g_Z	16.182382	16.349347
7	g_X	0.052614	0.078697
	g_Y	0.104875	0.143873
	g_Z	19.152827	19.101136
8	g_X	0.010394	0.011951
	g_Y	0.028583	0.028823
	g_Z	19.585273	19.578925

Table S8. Energies of the lowest Kramers doublets (cm^{-1}) of Dy ions in compound **5**.

Spin-orbit energies, cm^{-1}	
Basis 1	**Basis 2**
0	0
80.951	86.596
120.816	126.400
161.348	164.370
188.647	193.086
206.204	206.499
280.283	272.572
430.479	434.115

Table S9. The *g* tensors of the lowest Kramers doublets (KD) of Dy ions in compound **5**.

KD		Basis 1 *g*	Basis 2 *g*
1	g_X	0.154124	0.124334
	g_Y	0.234657	0.197367
	g_Z	19.178718	19.192557
2	g_X	2.196953	2.082552
	g_Y	5.091121	4.821664
	g_Z	12.394139	12.351724
3	g_X	1.161494	0.795294
	g_Y	4.764731	4.330801
	g_Z	9.202294	9.874373
4	g_X	2.050024	2.014446
	g_Y	5.992884	4.995983
	g_Z	12.068506	12.806504
5	g_X	0.835585	1.241896
	g_Y	2.523651	4.287891
	g_Z	11.244224	10.390331
6	g_X	1.900060	2.019966
	g_Y	2.937619	3.955402
	g_Z	14.789561	13.817800
7	g_X	0.069623	0.120948
	g_Y	0.137135	0.241182
	g_Z	19.205400	19.131610
8	g_X	0.004392	0.004807
	g_Y	0.007797	0.008305
	g_Z	19.677557	19.659381

Table S10. Energies and $<S^2>$ values obtained from BS-DFT in **1**-**5** complexes.

1	Gd	Fe	Gd	Fe	Energy, Ha	$<S^2>$
HS	↑	↑	↑	↑	-29462.064960	156.0217
BS1	↓	↑	↑	↑	-29462.065019	37.0194
BS2	↑	↓	↑	↑	-29462.065997	60.9971
BS3	↑	↓	↑	↓	-29462.065068	16.0173
BS4	↓	↓	↑	↑	-29462.066013	11.9968
BS5	↓	↑	↑	↓	-29462.065982	11.9973

2	Gd	Fe	Gd	Fe	Energy, Ha	$<S^2>$
HS	↑	↑	↑	↑	-29329.351997	156.0217
BS1	↓	↑	↑	↑	-29329.352021	37.0198
BS2	↑	↓	↑	↑	-29329.352666	61.0024
BS3	↑	↓	↑	↓	-29329.352046	16.0179
BS5	↓	↑	↑	↓	-29329.352664	12.0023

3	Gd	Fe	Gd	Fe	Energy, Ha	$<S^2>$
HS	↑	↑	↑	↑	-29011.891183	156.0217

BS1	↓	↑	↑	↑	-29011.891202	37.0197
BS2	↑	↓	↑	↑	-29011.892136	60.9989
BS3	↑	↓	↑	↓	-29011.891221	16.0178
BS4	↓	↓	↑	↑	-29011.892168	11.9986
BS5	↓	↑	↑	↓	-29011.892109	11.9991

4	Gd	Fe	Gd	Fe	Energy, Ha	$<S^2>$
HS	↑	↑	↑	↑	-30002.696634	156.0217
BS1	↓	↑	↑	↑	-30002.696657	37.0197
BS2	↑	↓	↑	↑	-30002.697373	61.0008
BS3	↑	↓	↑	↓	-30002.696680	16.0177
BS4	↓	↓	↑	↑	-30002.697370	12.0011
BS5	↓	↑	↑	↓	-30002.697376	12.0005

5	Gd	Fe	Gd	Fe	Energy, Ha	$<S^2>$
HS	↑	↑	↑	↑	-29011.902582	156.0215
BS1	↓	↑	↑	↑	-29011.902644	37.0194
BS2	↑	↓	↑	↑	-29011.903646	60.9985
BS3	↑	↓	↑	↓	-29011.902701	16.0174
BS4	↓	↓	↑	↑	-29011.903645	11.9986
BS5	↓	↑	↑	↓	-29011.903647	11.9984

Experimental magnetic properties

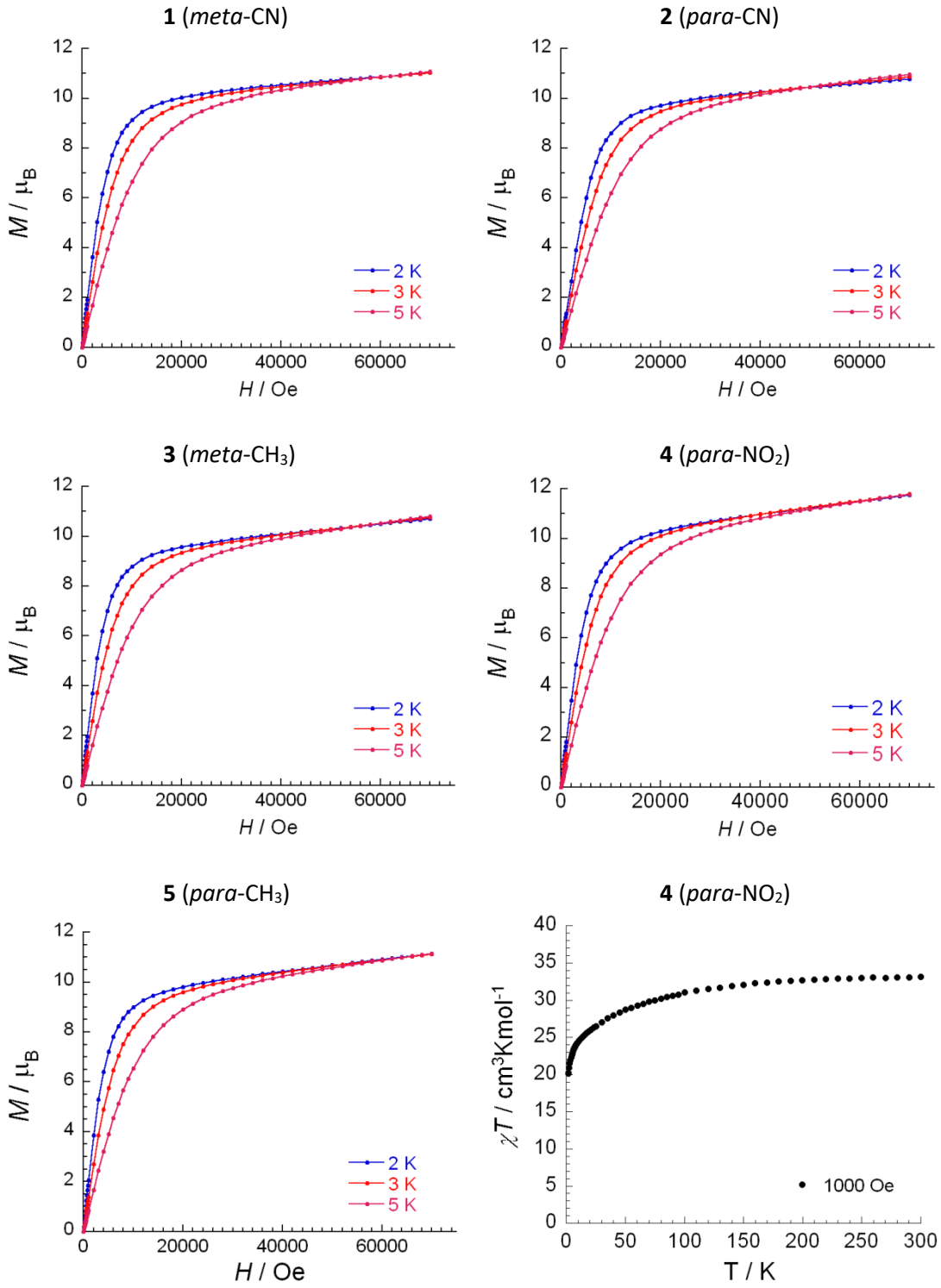

Figure S1. Field dependency of magnetization for **1**-**5**, and plot of χT v T for **4**

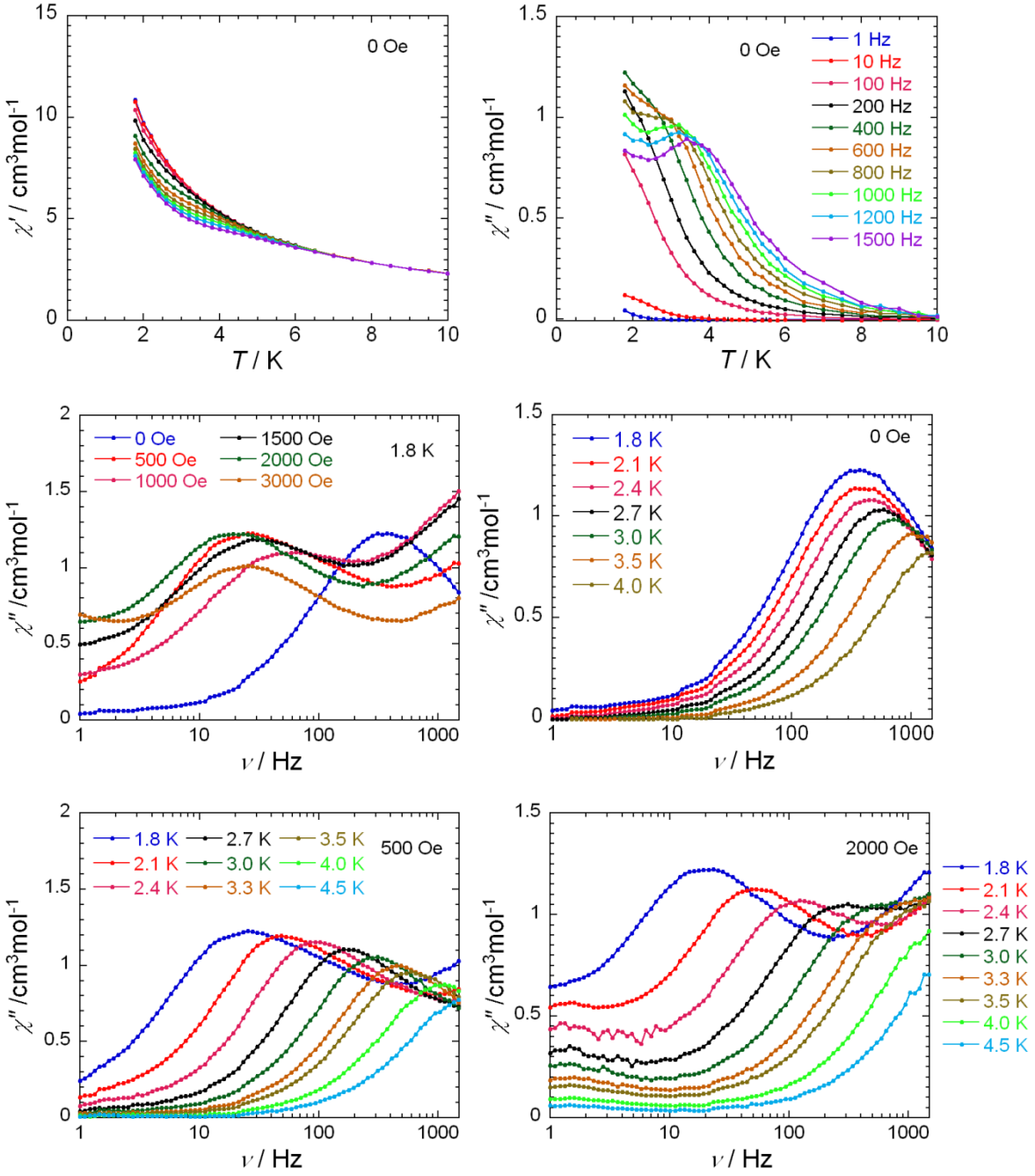

Figure S2. ac susceptibility data for **4:** T-dependence of χ' and χ" (upper two plots), frequency-dependence of χ" at 1.8K under different applied dc fields (centre row, left), frequency dependence of χ" over the temperature range 1.8-4.5 K in zero dc field (centre row, right) and under dc fields of 500 and 2000 Oe (bottom row).

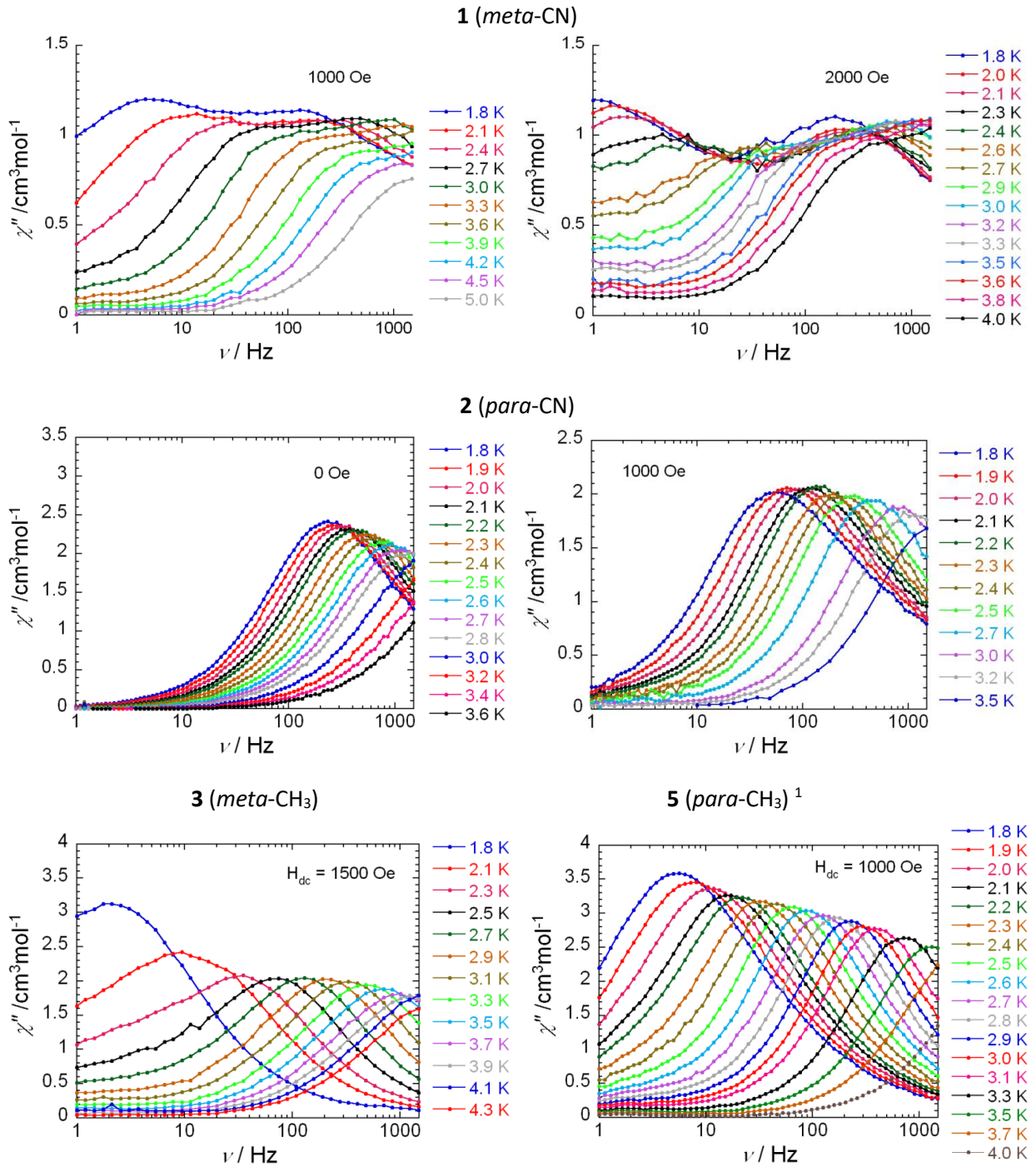

Figure S3. frequency-dependence of χ" for **1** under dc fields of 1000 and 2000 Oe (top row), for **2** under zero and 1000 Oe dc fields (middle row), for **3** under 1500 Oe cd field (bottom left) and for **5** under 1000 Oe dc field [1] (bottom right).

[1] A. Baniodeh et al. Chem. Comm., **2013**, *49*, 9666.

Ab initio calculated field-dependent magnetization

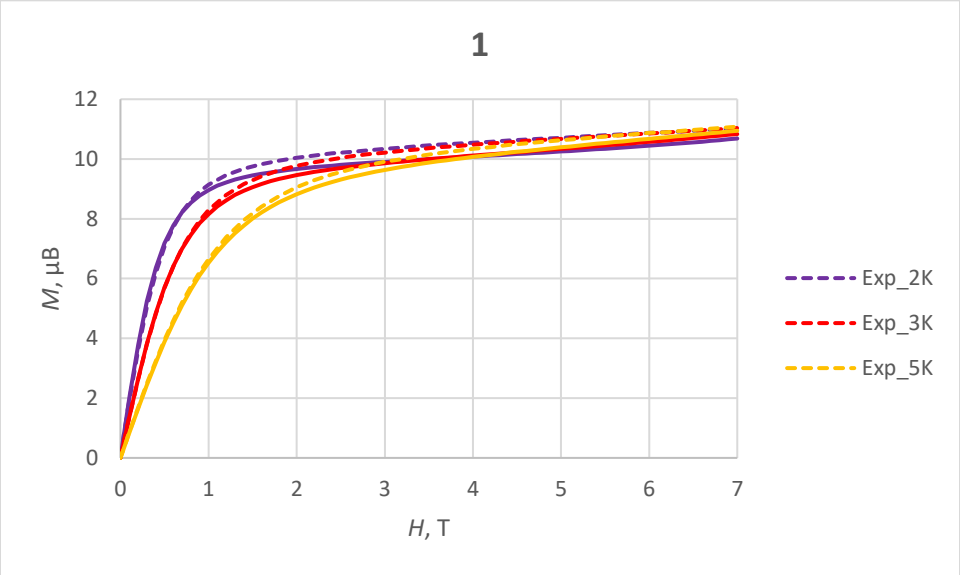

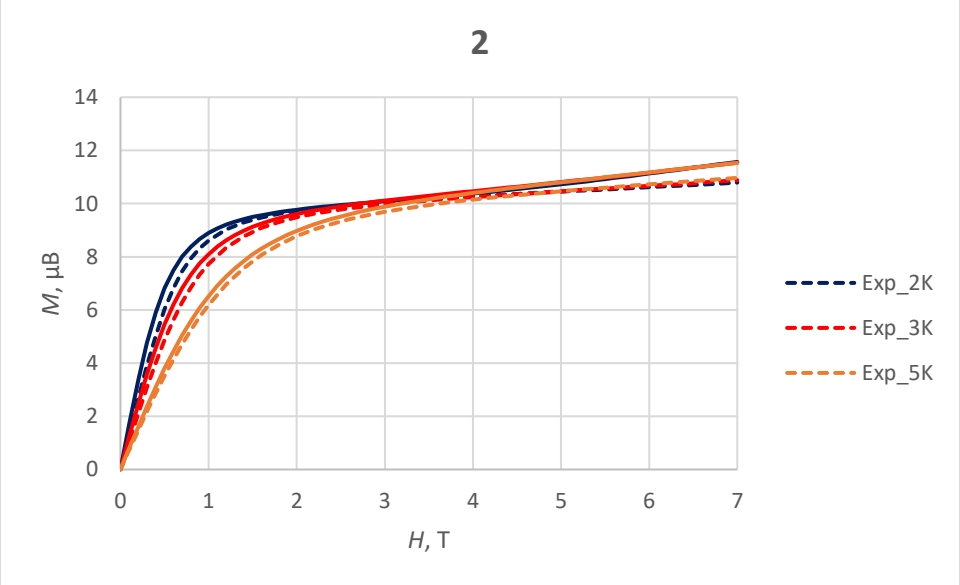

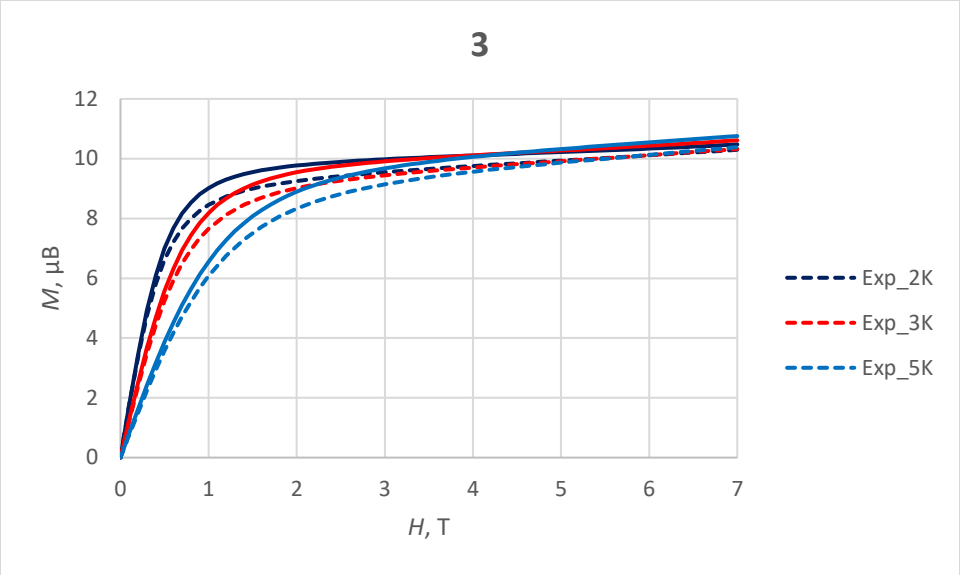
3
12
10
8
6
4
2
0
M, μB
0
1
2
3
4
5
6
7
H, T
Exp_2K
Exp_3K
Exp_5K

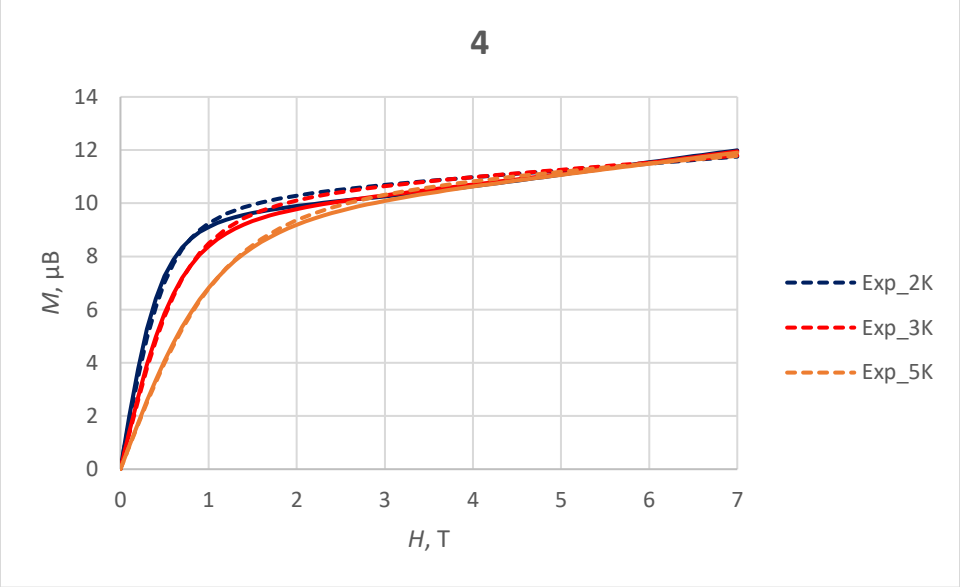
4
14
12
10
8
6
4
2
0
M, μB
0
1
2
3
4
5
6
7
H, T
Exp_2K
Exp_3K
Exp_5K

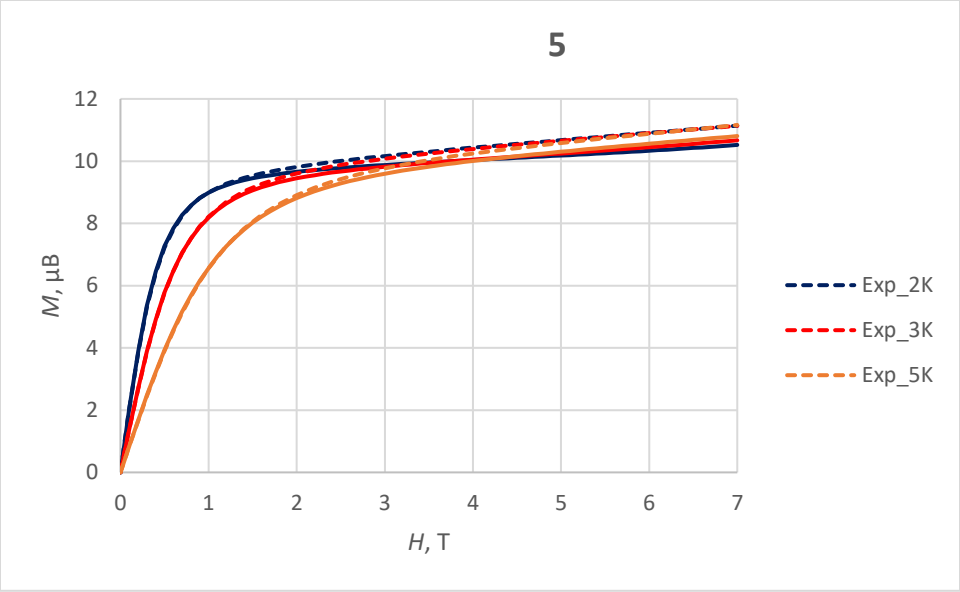

Figure S4. Experimental (dashed lines) vs. calculated (solid lines) static magnetization data for **1**-**5**.

EPR spectroscopy

The EPR spectra of compound **2** in X-band are shown in Figure S5. The broad absorption line detected at T = 4-15 K is similar to EPR spectrum of the polycrystalline sample with paramagnetic center with S = 1/2 or S = 1 with small ZFS for so-called parallel orientation, i.e. spectrum from the small crystals for which the external magnetic field is directed along g_z. The absence of signals for perpendicular orientations in the range of the external field up to 12000 Oe is associated with small values of $g_{x,y}$. The weak intensity of the observed signal is also a consequence of small $g_{x,y}$ values.

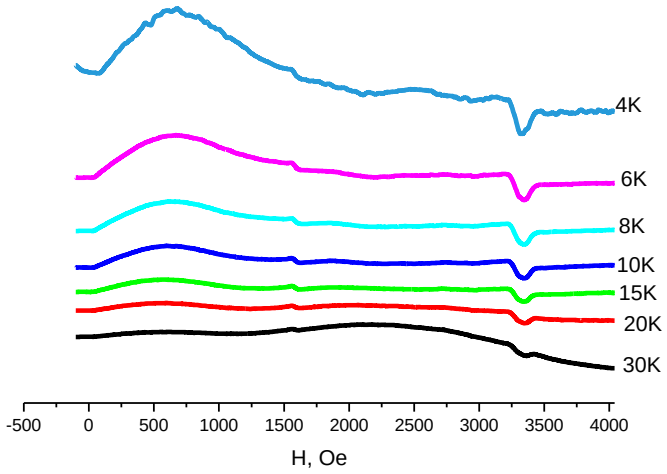

Figure S5. EPR spectra of compound **2** in X-band (ν=9.398GHz).

A similar spectrum in the X-band at T = 4-6K was observed for compound **5** (Figure 13a, main text).

The spectra of **1** and **4** in the X-band at low temperatures have another shape (Figures S6-7).

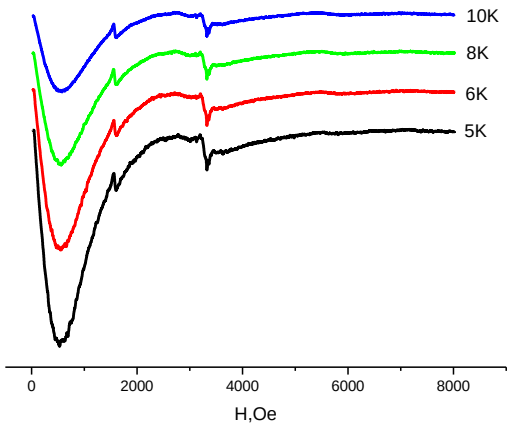

Figure S6. The temperature dependence of EPR spectrum of the polycrystalline sample of **1** in the X-band (ν=9.399GHz).

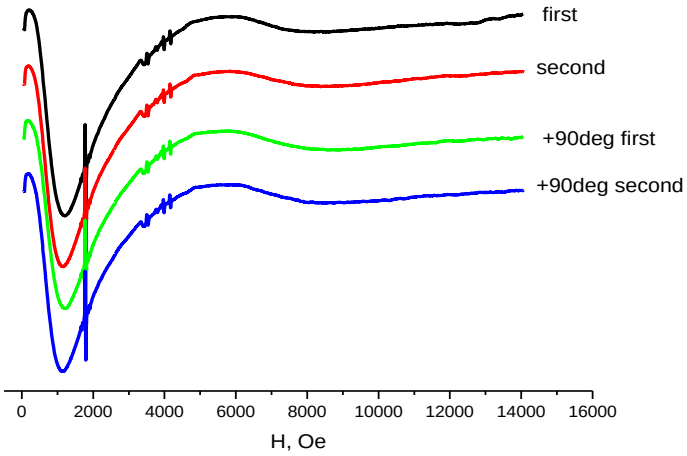

Figure S7. The of EPR spectrum of the polycrystalline sample of **4** at T=5K in the X-band (ν=9.766GHz). "first" – the first recording of the spectrum without prior effect of the magnetic field, "second" – the second recording of the spectrum after the sample is subjected to the effect of the external magnetic field. "90 deg" corresponds to the measurement when the ampoule was rotated by 90 degrees to avoid possible orientation of the crystals.

The EPR study of Dy_2Fe_2 clusters has shown that the shape of the EPR spectrum changes after the compound is subjected to the effect of the external magnetic field, especially in the Q- and W-bands (Figure S8). This change can be described by the appearance of some ordering as it indicates that the number of clusters with g_z oriented along external magnetic field increases after the effect of the external magnetic field.

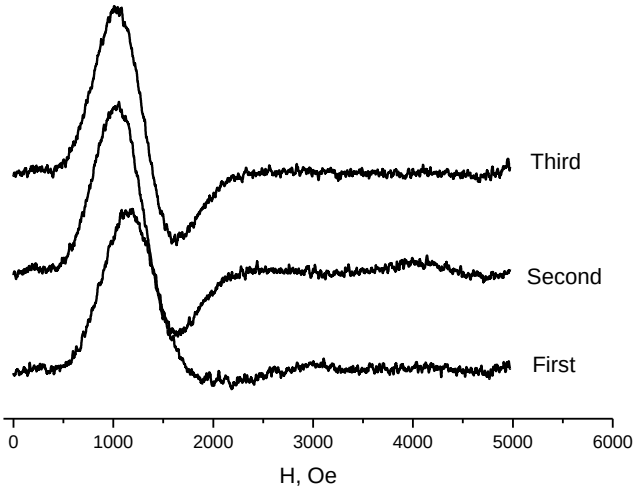

Figure S8. The EPR spectra of **1** at T=5K in the Q-band (ν=34.21GHz). The spectrum changes at second recording. "First", "Second" and "Third" corresponds to spectra for "first", 'second" and "third" of recordings, respectively.

We paid attention to the effect of the magnetic field in order to exclude it as much as possible in analyzing the EPR spectra. First recording of EPR spectra of **1**, **2**, **4** and **5** in Q band are shown in Figure S9. It should be noted that the observed shape of the spectrum in the X-band for **4** (Figure S7) is not a consequence of some ordering as in Figure S8.

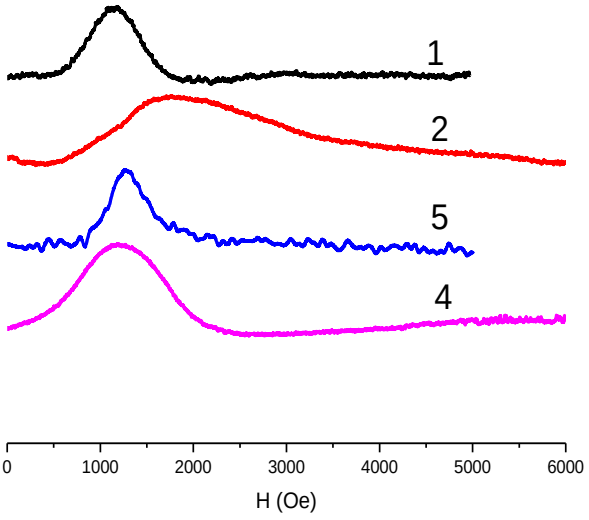

Figure S9. The EPR spectra of **1**, **2**, **4** and **5** at T= 5 K in the Q-band.

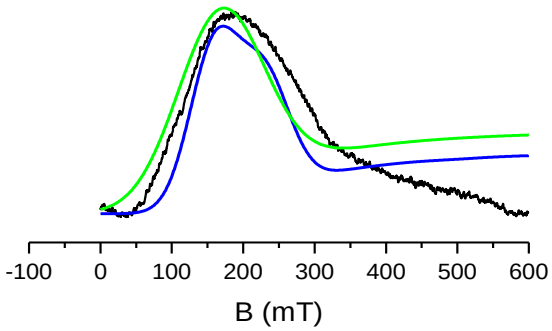

Figure S10. Experimental and simulated spectra of **2** in Q-band and T=5 K. Simulation parameter: blue line g_z=14.5, g_x=g_y =0.1 and J_{Ising}=0.4 cm^{-1}. Green line g_z=14.5, g_x =g_y =0.1 and J_{Ising}=0.1 cm^{-1}.